

## High Rate Capability of Fe/FeO/Fe<sub>3</sub>O<sub>4</sub> Composite as Anode Material for Lithium-Ion Batteries

L. Shi, Y.D. He, X.H. Xia, Z.M. Jian and H.B. Liu\*

*College of Materials Science and Engineering, Hunan University, Changsha Hunan 410082, China*

*(Received 10 July 2009, Accepted 1 November 2009)*

Fe/FeO/Fe<sub>3</sub>O<sub>4</sub> composite was synthesized by a simple solid method using ferric citrate and phenolic resin as raw materials. The reaction processes of raw materials mixture were characterized by thermogravimetric analysis (TGA) under nitrogen. X-Ray diffraction (XRD) and scanning electron microscopy (SEM) were used to investigate the structure and morphology of the products. The results showed that the obtained material was octahedral Fe/FeO/Fe<sub>3</sub>O<sub>4</sub> composite with a size of 2-4 μm. The electrochemical performances of Fe/FeO/Fe<sub>3</sub>O<sub>4</sub> composite as anode material were also evaluated, which exhibited a stable specific capacity of 260.3 mAh g<sup>-1</sup> and an ideal initial coulombic efficiency of 90.8% in the range of 0.05~3 V at the 5C rate. A good rate capacity of Fe/FeO/Fe<sub>3</sub>O<sub>4</sub> composite electrode was also shown by the charge-discharge testing even at the rate of 60C. The better rate capability of Fe/FeO/Fe<sub>3</sub>O<sub>4</sub> electrode could be measured in higher temperature.

**Keywords:** Fe/FeO/Fe<sub>3</sub>O<sub>4</sub> composite, High rate capability, Anode material, Lithium-ion batteries

---

### INTRODUCTION

In recent years, extraordinary efforts have been made to find alternative anodic materials to replace carbon-based materials, and various transition metal oxides with high capacity of lithium storage have been examined as promising anode electrode materials. Among these transition metal oxides, iron oxide is of particular interest due to its abundance, environmental friendliness, and low cost. Poizot group [1] and Taberna group [2] proposed FeO and Fe<sub>3</sub>O<sub>4</sub> as anode material for lithium-ion batteries, respectively. The FeO can reach a capacity of about 600 mAh g<sup>-1</sup>, and the Fe<sub>3</sub>O<sub>4</sub> possess a capacity of more than 800 mAh g<sup>-1</sup>. As the most stable iron oxide, hematite (α-Fe<sub>2</sub>O<sub>3</sub>) with a capacity of more than 1000 mAh g<sup>-1</sup> has been also reported recently by a large number of researchers [3-10].

However, the use of iron oxides suffers from two major drawbacks. One is the large irreversible capacity in the first cycle. The origin of the large irreversible capacity is the formation and decomposition of Li<sub>2</sub>O, as well as the redox of Fe. The other fault is the poor rate capability for iron oxides, except Fe<sub>3</sub>O<sub>4</sub> and FeO, due to their poor electric conductivity. Hence, it is important to improve the reversible decomposition of Li<sub>2</sub>O and the electric conductivity for iron oxides.

Since the main electrochemical irreversible behavior of iron oxide is caused by the reaction between Fe and Li<sub>2</sub>O, synthesizing Li<sub>2</sub>O-iron oxide binary composite system, or Fe-iron oxide binary composite system, is a facile route to decreasing its irreversible capacity. However, the electrochemical performance of Li<sub>2</sub>O-iron oxide binary composite was not very satisfactory [11] due to the formation of lithium ferrate. Fe-iron oxide binary composite anode, especially Fe/Fe<sub>3</sub>O<sub>4</sub> composite, possesses not only excellent electric property, but also reversible electrochemical

---

\*Corresponding author. E-mail: shilei197907@126.com

performance. Whereas, the chemical instability of Fe/Fe<sub>3</sub>O<sub>4</sub> composite is more obvious than Li<sub>2</sub>O-iron oxide binary composite, its special capacity is lower than iron oxide and Li<sub>2</sub>O-iron oxide binary composite. Thus, Fe/Fe<sub>3</sub>O<sub>4</sub> is seldom used as an anode material for lithium-ion batteries.

With the emergence of electric vehicles (EVs) and hybrid electric vehicles (HEVs), the high rate capacity of lithium-ion batteries has attracted special attention. The Fe-Fe<sub>3</sub>O<sub>4</sub> binary composite should be mentioned again for its high rate capability. In this paper, we have focused on a chemical steady Fe/FeO/Fe<sub>3</sub>O<sub>4</sub> composite. The electrochemical properties of Fe/FeO/Fe<sub>3</sub>O<sub>4</sub> composite anode have also been investigated.

## EXPERIMENTAL

### Material Preparation and Characterization

In a simple synthesis process, Fe/FeO/Fe<sub>3</sub>O<sub>4</sub> composite was synthesized *via* a solid route. 8.8 g phenolic resin (C.P., Changsha Zhida Co., China) and 83.8 g ferric citrate (A.R., Tianjin Guangfu Co., China) were dissolved in 36 ml ethanol (A.R., Changsha Huihong Co., China) by magnetic stirring. The slurry was dried at 80 °C for 2 h and then at 120 °C for 1 h. The Fe/FeO/Fe<sub>3</sub>O<sub>4</sub> composite was obtained by sintering the above uniform mixture at 750 °C for 12 h in an inert atmosphere.

XRD patterns were collected for Fe/FeO/Fe<sub>3</sub>O<sub>4</sub> composite on a D8-ADVANCE diffractometer (Brooke, Germany) with Cu-K $\alpha$  radiation (40 kV, 300 mA,  $\lambda = 1.54059 \text{ \AA}$ ), and the data were obtained at  $2\theta$  range of 10~70° with a scan rate of 0.02°/s. The SEM for Fe/FeO/Fe<sub>3</sub>O<sub>4</sub> composite was performed on a JSM-6700F (Hitachi, Japan). Thermogravimetric (TG) analysis was employed to evaluate the weight loss of the samples under a 20 ml min<sup>-1</sup> N<sub>2</sub> gas flow with a heating rate of 10 °C min<sup>-1</sup> using a thermal analyzer (STA449C, Netzsch, Germany).

### Electrochemical Measurements

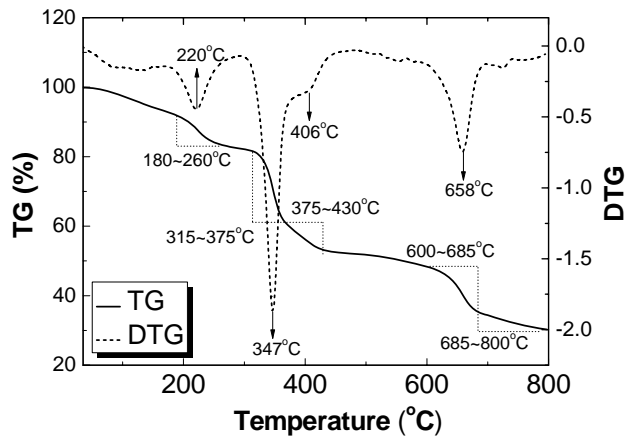
Electrode was typically prepared by coating a slurry of 70 wt% active material, 20 wt% acetylene black used as conductivity agent and 10 wt% poly-(vinylidene fluoride) (PVDF) as binder dissolved in n-methyl pyrrolidone (NMP) onto a Cu foil substrate. A pure lithium foil was used as counter and reference electrode, and the electrolyte (A.R.,

Shenzhen Zhubang Co., China) was 1 M LiPF<sub>6</sub> dissolved in ethylene carbonate/diethyl carbonate/dimethyl carbonate (EC:DEC:DMC = 1:1:1 Vol.). The separator was a micro-porous polypropylene film (Celgard 2300). The cells were assembled in an argon-filled glove box. The discharge/charge tests of Fe/FeO/Fe<sub>3</sub>O<sub>4</sub> octahedral composite at 5C and 60C were measured on a Land series CT-2001A battery test instrument (Wuhan Jinnuo Co., China). Both the Cycle voltammograms (CV) and ac impedance were measured with an electrochemical workstation (CHI660A, Shanghai Chenhua Co., China). The CV measurement was conducted over the potential range of 0~3V *vs.* Li/Li<sup>+</sup> at a scan rate of 0.1 mV s<sup>-1</sup>. Prior to ac impedance measurements, the electrode was held at a fixed potential for at least 2 h to attain the condition of sufficiently low residual current. Electrochemical impedance spectroscopy (EIS) was carried out by applying ac amplitude of 5 mV over the frequency range of 100 kHz to 1 Hz.

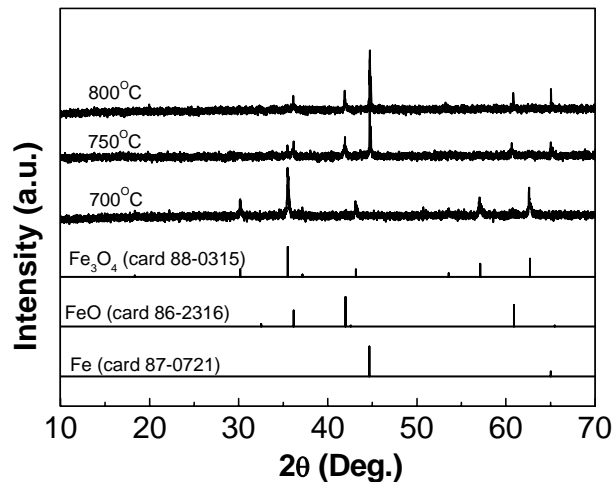
## RESULTS AND DISCUSSION

Figure 1 presents the TG and DTG curves for a mixture of iron citrate and phenolic resin. Four weight loss peaks around 220 °C, 347 °C, 406 °C and 658 °C can be distinctly observed in the DTG curve. The corresponding region of weight loss appearing in TG curve follow a sequence of 180~260 °C, 315~375 °C, 375~430 °C and 600~685 °C. Based on these, we may conclude that the first two weight losses are caused by the evaporation of crystal water in iron citrate and the decomposition of iron citrate, respectively. The weight loss at 406 °C is due to the pyrolysis of phenolic resin. The last weight loss occurring at 658 °C is the combined action of the carbonization process and the redox reaction of Fe<sup>3+</sup> with active carbon, which is obtained from the pyrolysis of phenolic resin.

The XRD patterns of the as-prepared samples and heat-treated at 700 °C, 750 °C and 800 °C for 12 h are presented in Fig. 2. The card patterns of Fe<sub>3</sub>O<sub>4</sub> (JCPDS card NO. 88-0315), FeO (JCPDS card NO. 86-2316) and metallic iron (JCPDS card NO. 87-0721) are also shown in this figure. The positions of the characteristic peaks of the product synthesized at 700 °C were consistent with the standard values for the Fe<sub>3</sub>O<sub>4</sub>. However, the peaks assigned to Fe and FeO



**Fig. 1.** TG and DTG curves for the mixture of iron citrate and phenolic resin.



**Fig. 2.** The XRD patterns of the samples obtained by heat-treating the mixture of phenolic resin and ferric citrate at different temperature.

were detected for the sample that was synthesized at 800 °C. Thus, the suitable heat treatment temperature for obtaining Fe/FeO/Fe<sub>3</sub>O<sub>4</sub> composite may be in the range of 700~800 °C. Weak and broad peaks of Fe<sub>3</sub>O<sub>4</sub>, FeO and Fe were all observed for the sample obtained at 750 °C. The typical peaks at 44.78° and 65.03° are attributed to the diffraction of (110) and (200) for Fe, the peaks at 36.07°, 41.91° and 60.65° correspond to the diffraction of (333), (600) and (660) for FeO, and the diffraction peak at 35.43° (311) is attributed to Fe<sub>3</sub>O<sub>4</sub>.

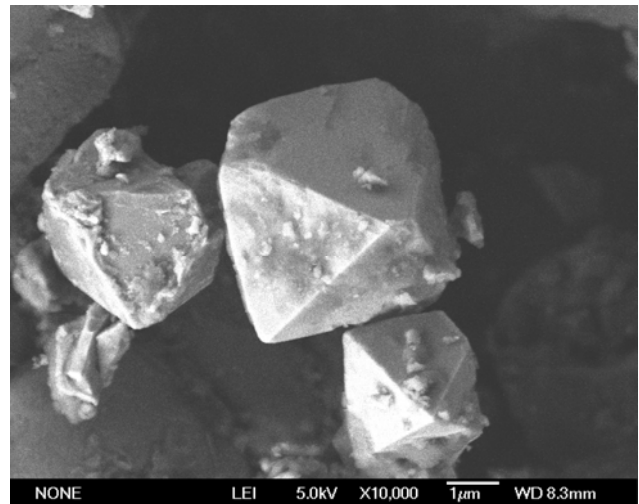


**Fig. 3.** SEM image of the Fe/FeO/Fe<sub>3</sub>O<sub>4</sub> composite.

The composite must also contain a few active carbons though its diffraction peaks could not be detected in the XRD pattern, because a slight weight loss at above 658 °C was detected in the TG curve shown in Fig. 1. Considering that the carbon content is relatively low, we would like to categorize the as-prepared product as Fe/FeO/Fe<sub>3</sub>O<sub>4</sub> ternary composite.

The SEM image revealed the morphology of Fe/FeO/Fe<sub>3</sub>O<sub>4</sub> composite, as shown in Fig. 3, which is clearly a crystal with quasi-octahedral structure. The framework of the particle is similar to Fe<sub>3</sub>O<sub>4</sub> with inverse spinel structure, indicating that the interior of the particle is Fe<sub>3</sub>O<sub>4</sub>, while the outer part mainly consists of Fe and FeO.

The charge-discharge tests were performed at room temperature and the first, second and third discharge/charge profiles of Fe/FeO/Fe<sub>3</sub>O<sub>4</sub> anode at 5C between 0.05 and 3V (vs. Li/Li<sup>+</sup>) are demonstrated in Fig. 4. During the first discharge process, a flat slope corresponding to the reaction of FeO and Fe<sub>3</sub>O<sub>4</sub> is observed below 1.0 V (vs. Li/Li<sup>+</sup>). The electrochemical equation for this reaction could be expressed as follows: Fe<sub>x</sub>O<sub>y</sub> + 2yLi<sup>+</sup> + 2ye<sup>-</sup> = xFe + yLi<sub>2</sub>O [12]. The slope in the first charge process is attributed to the decomposition of Li<sub>2</sub>O accompanying the oxidation of Fe which occurs within 1.5~2.1 V (vs. Li/Li<sup>+</sup>) [1,2,13]. In the subsequent 2nd and 3rd cycles, the discharge plateau increased markedly to 1.1 V (vs. Li/Li<sup>+</sup>), and the charge plateau also increased slightly,

indicating that the pristine Fe/FeO/Fe<sub>3</sub>O<sub>4</sub> electrode was charged somewhat during the first electrochemical cycle [1]. A discharge capacity of 286.5 mAh g<sup>-1</sup> was obtained in the first cycle with an irreversible capacity of 26.2 mAh g<sup>-1</sup> and the initial coulombic efficiency of 90.8%. The value of coulombic efficiency was far higher than the nanosized  $\alpha$ -Fe<sub>2</sub>O<sub>3</sub> electrode [3~10], suggesting that the ternary composite anode had a satisfactory electrochemical reversible property. In the following 2nd and 3rd cycles, the reversible capacities were determined to be 252.9 and 241.8 mAh g<sup>-1</sup> with coulombic efficiencies of 90.2 and 92.2%, respectively. The reversible capacity was gradually reduced in the first three discharge/charge cycles, which may be owing to the formation of SEI membrane on the Fe surface [14].

Cycling properties of the Fe/FeO/Fe<sub>3</sub>O<sub>4</sub> composite anode at room temperature at the rate of 5C and 60C are shown in Fig. 5. The electrode was cycled first at 5C rate for 30 cycles followed by a higher rate at 60C. The electrode retained a reversible capacity of more than 177 mAh g<sup>-1</sup> and 99 mAh g<sup>-1</sup> after 30 electrochemical cycles at the rate of 5C and 60C, respectively. The cycling is still going on in our laboratory. These results show that the obtained Fe/FeO/Fe<sub>3</sub>O<sub>4</sub> composite possesses an ideal cycling property even at big current densities.

Temperature dependence of the Nyquist plots for Fe/FeO/Fe<sub>3</sub>O<sub>4</sub> anode at a potential of 0.5 V is shown in Fig. 6. The high-frequency limit shifted to the negative direction on the real axis as the temperature increased, suggesting that the ohmic resistance, mainly the solution resistance of the electrolyte, decreased with increasing the cell temperature. This is associated with the increase in the electrolyte conductivity, the increase in viscosity and good wettability of the electrolyte with Fe/FeO/Fe<sub>3</sub>O<sub>4</sub> materials at high temperatures. All plots exhibit two depressed semicircles at high and intermediate frequency regions, which are attributed to the charge-transfer processes for FeO and Fe<sub>3</sub>O<sub>4</sub>, respectively. The overall impedance for the high-to-medium frequency semicircles decreases swiftly with a decreasing temperature. The higher internal resistance at a low temperature produces large potential hysteresis. From this point of view, the increasing IR drop for the electrochemical cycling carried out between 0.05-3 V cut-off voltage is thus an important factor leading to the low reversible capacity of the

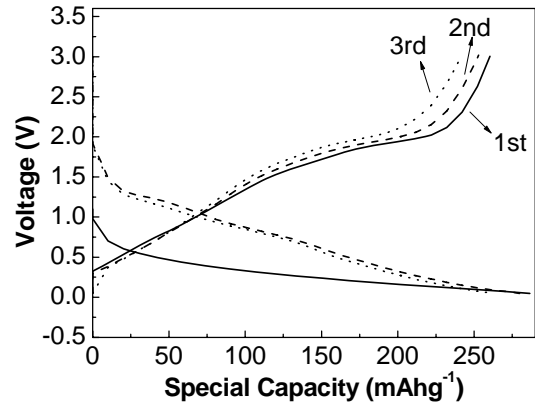


**Fig. 4.** The first three discharge-charge curve of Fe/FeO/Fe<sub>3</sub>O<sub>4</sub> composite anode at a rate of 5C between 0.05~3 V.

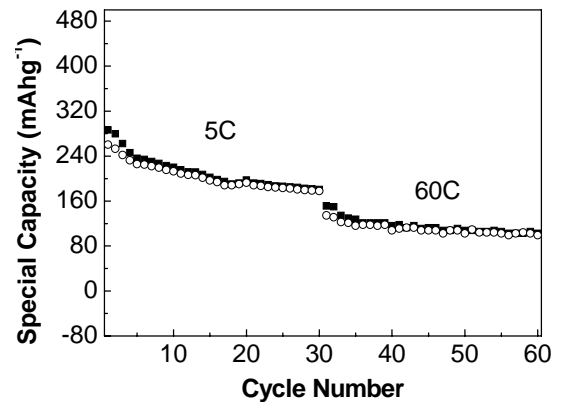


**Fig. 5.** The cycle performance of Fe/FeO/Fe<sub>3</sub>O<sub>4</sub> composite anode at rates of 5C and 60C between 0.05~3 V.

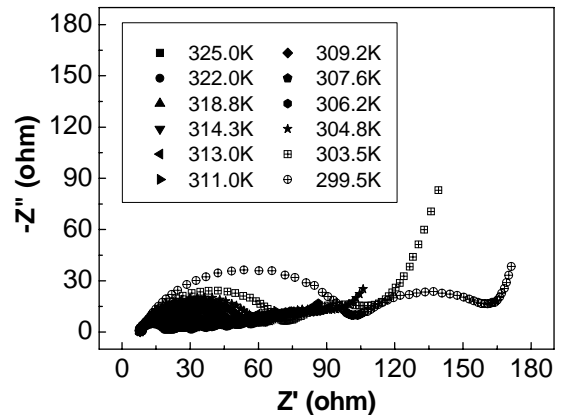


**Fig. 6.** The influence of the cell temperature on the Nyquist plot of Fe/FeO/Fe<sub>3</sub>O<sub>4</sub> composite anode between 299.5~325.0 K.

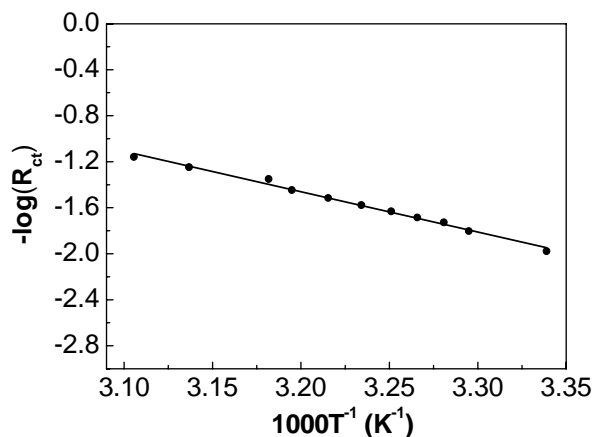


Fig. 7. An Arrhenius plot of  $R_{ct}^{-1}$  obtained from the Nyquist plots shown in Fig. 5.

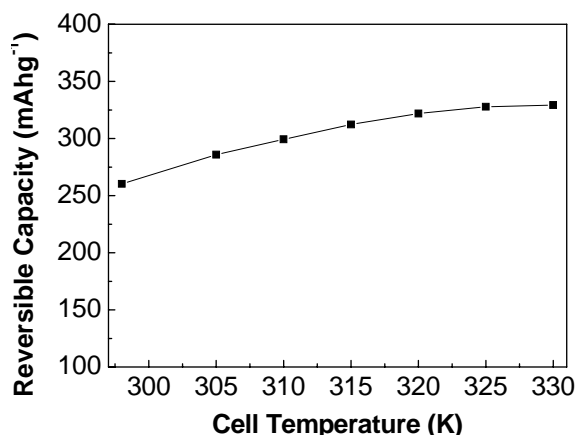


Fig. 8. The influence of the cell temperature on the first reversible capacity of Fe/FeO/Fe<sub>3</sub>O<sub>4</sub> composite anode between 298–330 K.

Fe/FeO/Fe<sub>3</sub>O<sub>4</sub> anode at the cell-test-temperature of 298 K. Moreover, shrinkage of the two semicircles with increasing temperature shows that all the reaction steps of the lithium intercalation are thermally activated processes. The plots also contain a straight line in low frequencies, which describes the response of the system to a semi-infinite diffusion of lithium ion through the Fe/FeO/Fe<sub>3</sub>O<sub>4</sub> electrode.

The activation energy for the interfacial lithium ion transfer at 0.5 V was evaluated from the temperature

dependence of the charge transfer resistances as shown in Fig. 7. The Arrhenius plot of  $1/R_{ct}$  with good linearity was observed, and the average value of the apparent activation energy for each charge transfer, calculated from the angle of the plot, was  $33 \pm 2$  kJ mol<sup>-1</sup>. This value is slightly higher than that of carbon materials, which means that the influence of the cell temperature on Fe/FeO/Fe<sub>3</sub>O<sub>4</sub> was greater than that of carbon materials, and the better rate capability of Fe/FeO/Fe<sub>3</sub>O<sub>4</sub> electrode was measured in higher temperatures as shown in Fig. 8.

## CONCLUSIONS

A simple solid route was adopted to prepare the Fe/FeO/Fe<sub>3</sub>O<sub>4</sub> composite. The electrochemical tests for the Fe/FeO/Fe<sub>3</sub>O<sub>4</sub> composite were performed on the lithium ion semi-batteries. This anode material exhibited an ideal initial coulombic efficiency of 90.8% at the 5C rate and a high rate capacity at the rate of 60C. Its activation energy for the interfacial lithium ion transfer at 0.5 V was  $33 \pm 2$  kJ mol<sup>-1</sup>, indicating that the better rate capability of the Fe/FeO/Fe<sub>3</sub>O<sub>4</sub> electrode could be measured in higher temperatures. We hope that these findings would help pave the way for the use of conversion reaction electrodes in future-generation lithium ion batteries.

## REFERENCES

- [1] P. Poizot, S. Laruelle, S. Grugeon, Nat. 407 (2000) 496.
- [2] P.L. Taberna, S. Mitra, P. Poizot, P. Simon, J.M. Tarascon, Nat. Mat. 5 (2006) 567.
- [3] J.J. Xu, G. Jain, Electrochem. Solid-State Lett. 6 (2003) A190.
- [4] T. Matsunura, N. Sonoyama, R. Kanno, M. Takano, Solid State Ionics 158 (2003) 253.
- [5] S.H. Zhan, D.R. Chen, X.L. Jiao, S.S. Liu, J. Colloid Interface Sci. 308 (2007) 265.
- [6] G. Jain, M. Balasubramanian, J.J. Xu, Chem. Mater. 18 (2006) 423.
- [7] H. Morimoto, S.I. Tobishima, Y. Lizuka, J. Power Sources 146 (2005) 315.
- [8] K. Woo, H.J. Lee, J. Magn. Mater. 272-276

- (2004) e1155.
- [9] K. Kandori, T. Ishikawa, J. Colloid Interface Sci. 272 (2004) 246.
- [10] L.L. Wang, J.S. Jiang, Physica B 390 (2007) 23.
- [11] P.C. Wang, H.P. Ding, T. Bark, Electrochimica Acta 52 (2007) 6650.
- [12] L. Wang, Y. Yu, P.C. Chen, D.W. Zhang, C.H. Chen, J. Power Sources 183 (2008) 717.
- [13] D.W. Zhang, C.H. Chen, J. Zhang, F. Ren, Chem. Mater. 17 (2005) 5242.
- [14] Y.N. NuLi, R. Zeng, P. Zhang, Z.P. Guo, H.K. Liu, J. Power Sources 184 (2008) 456.